Optical Model for Diffractive Resonance Excitation*

M. Elitzur†
The Rockefeller University, New York, New York 10021

and

R. G. Lipes
Carnegie-Mellon University, Pittsburgh, Pennsylvania 15213
(Received 19 October 1972)

An optical model of the Chou-Yang type has been extended to treat resonance production in high-energy pp scattering. Dipole form factors have been used for the hadronic matter distribution. Good qualitative agreement with experiment is found for differential elastic and single-excitation cross sections for momentum transfers out to 2–3 GeV^2.

I. INTRODUCTION

One of the successful approaches to high-energy pp elastic scattering is that of Chou and Yang[1] in which it is assumed that elastic scattering reflects the absorption due to all open channels. The hadrons are viewed as extended objects of absorbing matter with a distribution described by a form factor. Since this picture does not arise from any fundamental theory, the theoretical input is the particular function chosen for the form factor, which usually is taken to be the electromagnetic one. Parametrizing the form factor with the empirical dipole fit and performing the complete impact-parameter transform,[2] one can account very well for the general features of the data, including the presence of dips and the value of the forward slope. This success is not meaningless since changes in the value of the dipole mass can make the dips disappear altogether (see Sec. II below). On account of this success, one is encouraged to extend the idea to other diffractive processes such as resonance excitation. Association of the $N \to N^*$ transition form factor with the electromagnetic excitation form factor leads to a scaling relation between elastic scattering and resonance excitation that seems to explain quite well the $NN \to NN^*$ differential cross section in terms of NN elastic scattering.[3]

In this paper we will further pursue the above ideas by using the elastic dipole fit along with the scaling property of the form factor to obtain an explicit expression for the excitation form factors. In principle, this enables us to calculate the excitation cross sections directly. In practice, however, the coupling of elastic and resonant channels becomes very complicated if more than one resonance is involved, so we have confined ourselves to one resonance. The aim of this paper, therefore, is rather limited. We cannot hope to improve upon the calculation of the elastic scattering and in fact we are likely going to spoil it at large values of t where the coupling of more resonances is important in the higher terms of the Glauber expansion (Sec. IV). We would be content, therefore, if all the qualitative features of the data up to $|t| \simeq 2$–3 GeV^2 emerged. It is gratifying that this is the case, indeed. The elastic differential cross section has a dip while the excitation differential cross section does not.

The paper is organized as follows: In Sec. II, we present for completeness the treatment of elastic scattering decoupled from resonant channels (as was done in Ref. 2). We notice that the model gives a change in the forward slope in agreement with the ISR (CERN Intersecting Storage Rings) data.[4,5] In Sec. III, we describe the general formalism for the treatment of the coupled-channels problem. In Sec. IV we present the actual calculation for the case of one resonance coupled to the elastic channel and give results for elastic scattering as well as single- and double-resonance excitation. We conclude with a short discussion of the model's results.

II. ELASTIC SCATTERING

To treat high-energy elastic scattering of particles A and B at small angles,[1,2] we will assume the scattering is approximately spin-independent, so that we can write the scattering amplitude in the impact-parameter representation

$$f(s,t) = i\int_0^\infty [1 - S(b)]J_0(b\sqrt{-t}\,)b\,db\,, \tag{1}$$

where $S(b)$ is the S-matrix element at impact parameter b and the normalization is such that the differential cross section is given by

$$\frac{d\sigma}{dt} = \pi|f(s,t)|^2\,. \tag{2}$$

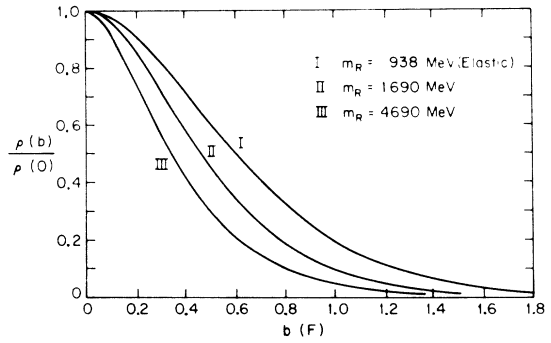

FIG. 1. The normalized density $\rho(b)/\rho(0)$ of Eq. (13) vs b with $\mu = \mu_0$ for $m_R = m$, the nucleon mass [which reduces to $\rho(b)/\rho(0)$ of Eq. (7)], $m_R = 1690$ MeV, and $m_R = 5m$, a fictitious large mass resonance.

Furthermore, we assume as in Ref. 1 that the near forward scattering is primarily due to strong, local absorption of the incident waves, with this absorption being proportional to the total amount of interpenetrating hadronic matter. This leads to

$$S(b) = e^{-\kappa\rho(b)}. \tag{3}$$

The density $\rho(b)$ is related to the form factors $G_A(t), G_B(t)$ of the hadronic matter distribution of particles A, B by

$$\rho(b) = \int_0^\infty G_A(t)G_B(t)J_0(b\sqrt{-t})\sqrt{-t}\, d(\sqrt{-t}). \tag{4}$$

At this point, we should emphasize that specification of the form factors $G_A(t), G_B(t)$ determines the model completely and provides the basic theoretical input. The absorption coefficient κ of Eq. (3) is a phenomenological parameter fixed through the optical theorem by the total cross section

$$\sigma_T = 4\pi \operatorname{Im} f(s, 0). \tag{5}$$

For proton-proton scattering we assume that the effective matter and charge distributions are identical and take for $G_A(t)$ the dipole fit to the charge form factor of the proton

$$G(t) = \left(1 - \frac{t}{\mu^2}\right)^{-2}, \tag{6}$$

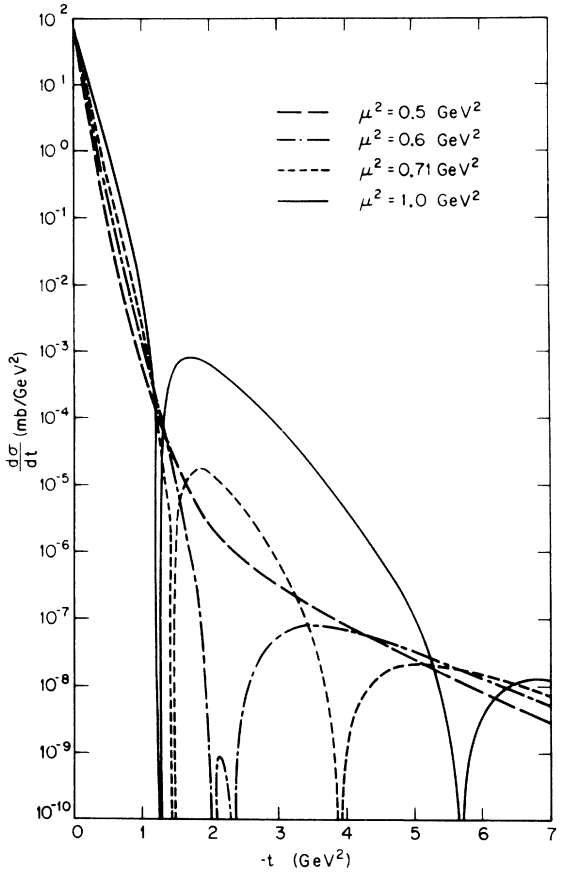

FIG. 2. Single-channel elastic $pp \to pp$ differential cross section $d\sigma/dt$ vs t using $\rho(b)$ of Eq. (7) with $\mu^2 = 0.5$ GeV^2, $\mu^2 = 0.6$ GeV^2, $\mu^2 = 0.71$ GeV^2, and $\mu^2 = 1.0$ GeV^2.

where electron scattering experiments suggest $\mu^2 = \mu_0^2 \equiv 0.71$ GeV^2. Equations (4) and (6) imply

$$\rho(b)/\rho(0) = \tfrac{1}{8}(\mu b)^3 K_3(\mu b), \quad \rho(0) = \tfrac{1}{6}\mu^2, \tag{7}$$

where K is the modified Bessel function. The normalized function $\rho(b)/\rho(0)$ is shown in Fig. 1 with $\mu = \mu_0$. Notice that $\rho(b)$ and, consequently, the scattering amplitude $1 - S(b)$ have the shape required of a diffractive amplitude in impact parameter space by Harari's absorption model.[6]

TABLE I. Experimental and theoretical values of slope parameter for elastic pp forward peak.

Range of $\lvert t\rvert$ (GeV^2)	Experimental slope parameter (GeV^{-2})	Theoretical slope parameter (GeV^{-2})
0.060–0.112	12.87 ± 0.20 ($s = 2013$ GeV^2)	12.1 for $\mu^2 = \mu_0^2$
	12.40 ± 0.30 ($s = 2808$ GeV^2)	9.3 for $\mu^2 = 1$ GeV^2
0.168–0.308	10.83 ± 0.20 ($s = 2013$ GeV^2)	10.5 for $\mu^2 = \mu_0^2$
	10.80 ± 0.20 ($s = 2808$ GeV^2)	8.6 for $\mu^2 = 1$ GeV^2

To obtain an expression for $S(b)$ we identify the matter and charge form factors. We can test the consistency of this hypothesis from the dependence of the differential cross section on μ, the dipole mass, appearing in Eq. (6). The curve for $d\sigma/dt$ vs t for various values of μ is shown in Fig. 2. Notice that no zeros are present for $\mu^2 \lesssim 0.6$ GeV^2, whereas two zeros occur for higher values. Presumably the dip in pp data at $t \approx -1.2$ GeV^2 (Refs. 7 and 8) arises from such a diffraction zero, so μ must be at least as great as μ_0.

The model predicts a slope for the very forward peak which changes around $-t \approx 0.1$ GeV^2.[5] The values of the slope parameter on either side of this change are presented in Table I for $\mu^2 = \mu_0^2$ and 1 GeV^2. As this is an asymptotic model we confront these values with the ISR data at the highest energy[4] and find $\mu^2 = \mu_0^2$ is favored.

We can calculate the total elastic cross section from the expression

$$\sigma_{el} = 2\pi \int_0^\infty |1 - S(b)|^2 b db . \tag{8}$$

With $\mu = \mu_0$ and $\sigma_T = 39$ mb (as we take throughout this paper) σ_{el} is approximately 20% of σ_T as suggested by present experimental data.

We see, therefore, that the Chou-Yang optical model can provide a consistent picture of pp elastic scattering when we use the dipole fit with $\mu = \mu_0$.

III. RESONANCE-EXCITATION FORMALISM

We describe resonance excitation in the model by specifying the form factor $G_R(t)$ which represents the possibility of a nucleon becoming an N^* and vice versa. We do not attempt to justify the procedure, but take it as a working hypothesis. One may think of it, for instance, as diffractive dissociation mediated by exchange of an infinitely heavy Pomeranchukon. Another framework in which it applies is the Glauber picture where $G_R(t)$ is related to the probability that a particle is excited to a higher state during interaction. In any case, from the initial NN state, many virtual states (such as NN^*, N^*N^*, etc.) may be reached during the course of the interaction, so the function $\kappa\rho(b)$ of elastic scattering must be replaced by a matrix $B(b)$. The possible intermediate states label the rows and columns in the usual manner. Every matrix element will be related to the appropriate form factors by a Bessel transform analogous to Eq. (4). The multichannel S matrix is given by

$$S(b) = e^{-B(b)} \tag{9}$$

with the exponentiation accounting for the coupling between communicating channels. The scattering amplitude again is related to $S(b)$ by Eq. (1) with the differential cross section for state j to be reached from state i given by

$$\frac{d\sigma_{ij}}{dt} = \pi |f_{ji}(s,t)|^2 . \tag{10}$$

As in elastic scattering, the only other theoretical input will be the form factors, as the absorption coefficients are determined by total excitation cross sections. The success of the electromagnetic form factors in incorporating features of elastic pp data tempts us to use the electromagnetic excitation form factor for diffractive $N \to N^*$ transitions. We can utilize the scaling property of inelastic electron scattering to write[3,9]

$$G_R(t, m_R^2) = G(t/m_R^2) \tag{11}$$

(where m_R is the resonance mass), so we have only one common form factor, the elastic one, when we scale the momentum transfer by the resonance mass squared. Relation (11), together with the assumption of factorization for the excitation cross section, was shown to lead to very good agreement with experimental data.[3] Also, one can somewhat understand this relation in a simpleminded parton picture of hadrons.[10] We will, therefore, adopt it for resonance excitation. If we take the dipole fit of Eq. (6), it follows that G_R is also given by a dipole with mass

$$\mu_R = \mu_0 \frac{m_R}{m} , \tag{12}$$

where m is the nucleon mass. We can now calculate the absorption density $\rho_R(b)$ from Eq. (4) to obtain

$$\rho_R(b) = C\left(\frac{4\mu^2\mu_R^2}{\mu_R^2 - \mu^2}[K_0(\mu_R b) - K_0(\mu b)] + \mu_R^2 \mu b K_1(\mu b) + \mu^2 \mu_R b K_1(\mu_R b)\right) , \tag{13}$$

$$C^{-1} = \frac{\mu^2}{1 - (m/m_R)^2}\left[2\ln\left(\frac{m^2}{m_R^2}\right) + \frac{m_R^4 - m^4}{m_R^2 m^2}\right] .$$

Figure 1 shows $\rho_R(b)$ as given by (13) plotted for $N^*(1690)$ and for a fictitious resonance with $m_R = 5m$. The excitation comes from the more central regions in impact-parameter space as the resonance produced becomes heavier. Clearly, this should be the case in view of the transform relation between $\rho(b)$ and the form factors [Eq. (4)], and the scaling relation (11).

To complete the specification of the matrix $B(b)$, we must deduce the form factors for the transitions $N^* \to N^*$. Here, of course, we cannot hope for an experimental hint and for simplicity will take them equal to the elastic $N \to N$ form factor.

IV. CALCULATION

The model outlined in the previous section enables one, in principle, to consider any number of resonances. In practice, the calculation becomes quite complicated for more than one resonance, so we will treat only the prominent $N^*(1690)$. With retention of a single resonance, we expect, *a priori*, that the calculation will only apply for $-t \lesssim 2$–3 GeV^2 for the following reason: At low values of t only the first few terms in the expansion of the exponential of Eq. (9) are important, but as $|t|$ increases so does the importance of higher terms and more resonances become coupled. From elastic scattering we know that the third-order terms become comparable to the lower ones at the second zero of Fig. 2 ($-t \approx 4$–5 GeV^2). We choose the $N^*(1690)$ since it is more strongly coupled and better separated experimentally from other resonances than are the lower diffractive states which are usually mixed with the $N^*(1238)$.[11]

The matrix $B(b)$ is now 4×4. We assume complete factorization in the momentum-transfer variable so that, not only is the t dependence given by a product of the form factors, but the absorption coefficients factorize as well. $B(b)$ will then have only three independent elements, B_{11}, B_{12}, and B_{22}:

$$B_{11} \equiv \langle NN|\, B\,|NN\rangle = \kappa_{11}\rho(b), \tag{14a}$$

$$B_{12} \equiv \langle NN^*|\, B\,|NN\rangle = \kappa_{12}\rho_R(b), \tag{14b}$$

$$B_{22} \equiv \langle N^*N^*|\, B\,|NN\rangle = \kappa_{22}\rho(b), \tag{14c}$$

where $\rho(b)$ for Eqs. (14a) and (14c) is given by Eq. (7) with $\mu = \mu_0$ and $\mu = \mu_R$, respectively, while $\rho_R(b)$ of Eq. (14b) is given by Eq. (13). The factorization assumption requires

$$\kappa_{11}\kappa_{22} = \kappa_{12}^{\,2}. \tag{15}$$

When we account for the Pauli principle in the intermediate states the compete matrix $B(b)$ becomes

$$B(b) = \begin{array}{c} \\ \langle NN| \\ \langle NN^*| \\ \langle N^*N| \\ \langle N^*N^*| \end{array} \begin{array}{c} \begin{array}{cccc} |NN\rangle & |NN^*\rangle & |N^*N\rangle & |N^*N^*\rangle \end{array} \\ \begin{bmatrix} B_{11} & B_{12} & -B_{12} & B_{22} \\ B_{12} & B_{11} & B_{22} & -B_{12} \\ -B_{12} & B_{22} & B_{11} & B_{12} \\ B_{22} & -B_{12} & B_{12} & B_{11} \end{bmatrix} \end{array}. \tag{16}$$

To exponentiate B we first diagonalize it. Noticing that B is of the form

$$\begin{pmatrix} M_1 & M_2 \\ M_2 & M_1 \end{pmatrix},$$

where M_1, M_2 are 2×2 matrices of the same form, we find the diagonalizing matrix U is

$$U = \frac{1}{2}\begin{pmatrix} T & T \\ T & -T \end{pmatrix} \quad \text{with} \quad T = \begin{pmatrix} 1 & 1 \\ 1 & -1 \end{pmatrix}. \tag{17}$$

Then we have

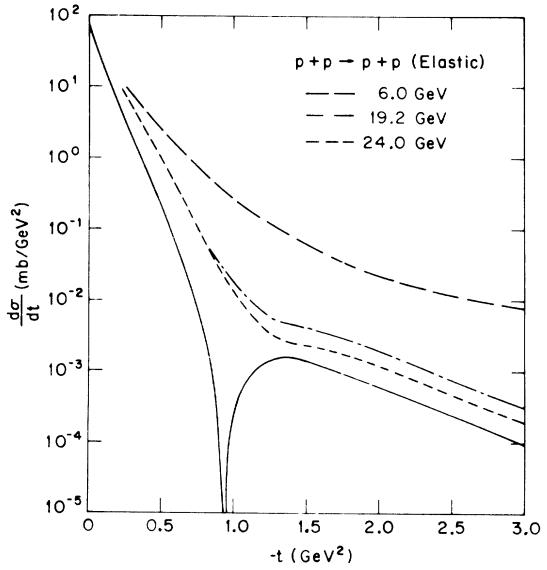

FIG. 3. Coupled-channel elastic $pp \to pp$ differential cross section $d\sigma/dt$ vs t. The experimental data are from Ref. 14.

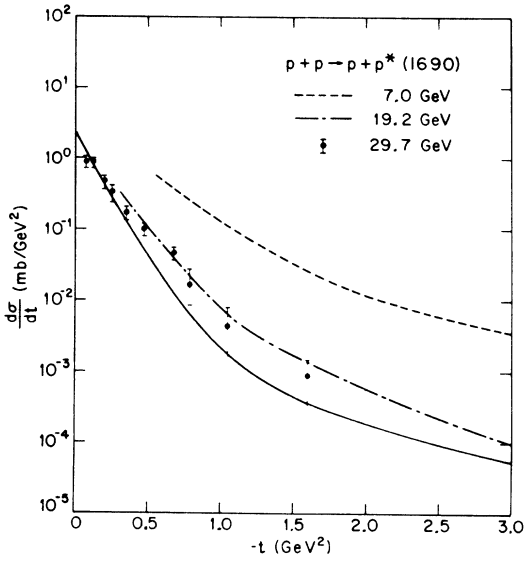

FIG. 4. Coupled-channel single-excitation $pp \to pp^*(1690)$ differential cross section $d\sigma/dt$ vs t. The experimental data are from Refs. 13 and 14.

$$UBU^{-1} = \begin{bmatrix} B_{11}+B_{22} & 0 & 0 & 0 \\ 0 & B_{11}-2B_{12}-B_{22} & 0 & 0 \\ 0 & 0 & B_{11}+2B_{12}-B_{22} & 0 \\ 0 & 0 & 0 & B_{11}+B_{22} \end{bmatrix} . \tag{18}$$

After exponentiation, the three independent S-matrix elements are

$$\langle NN|S|NN\rangle = \tfrac{1}{4}[2\exp(B_{11}+B_{22}) + \exp(B_{11}-2B_{12}-B_{22}) + \exp(B_{11}+2B_{12}-B_{22})] , \tag{19a}$$

$$\langle NN|S|NN^*\rangle = \tfrac{1}{4}[\exp(B_{11}+2B_{12}-B_{22}) - \exp(B_{11}-2B_{12}-B_{22})] , \tag{19b}$$

$$\langle NN|S|N^*N^*\rangle = \tfrac{1}{4}[2\exp(B_{11}+B_{22}) - \exp(B_{11}-2B_{12}-B_{22}) - \exp(B_{11}+2B_{12}-B_{22})] . \tag{19c}$$

We now have all that we need to calculate elastic scattering and single and double excitation; it remains to fix the two absorption coefficients κ_{11} and κ_{12}. Equation (5) and the corresponding relation for the total excitation cross section for $NN \to NN^*$,

$$\sigma_{\text{exc}} = 2\pi \int_0^\infty |\langle NN^*|S|NN\rangle|^2 b\,db , \tag{20}$$

define κ_{11} and κ_{12} implicitly. These two relations can be inverted by a simple numerical procedure[12] to solve for κ_{11} and κ_{12}.

The results of the computation are presented in Figs. 3, 4, and 5 (experimental data are taken from Refs. 13 and 14). Figure 3 gives the elastic scattering treated in the coupled-channel approach. Comparison with Fig. 2 shows that coupling to the resonance hardly affects the forward peak out to the first dip. This is expected since the first term in the expansion of the S matrix dominates in this region, so the channels are effectively decoupled. After the dip, however, the resonance contribution shifts the curve upwards, somewhat above the recent ISR results.[8] This shift demonstrates the increasing role the resonances are playing as t gets larger. We cannot hope, therefore, to get a good agreement for elastic scattering from the coupled-channels calculation unless we include many resonances. It is gratifying, however, that the most marked feature of pp elastic scattering, namely, the dip around $t \simeq -1.2$ GeV^2, does emerge from this simplified model. Figure 4 presents the results of single diffractive excitation. In contrast with the elastic case, the main feature of this curve is that no dip is present which agrees with present experimental data.[13] The slope parameter for the forward peak is significantly smaller than that of elastic scattering, again in agreement with experiment. Figure 5 shows the prediction for double excitation. The cross section for the process $NN \to N^*N^*$ is 0.07 mb, whereas straightforward factorization gives 0.04 mb.

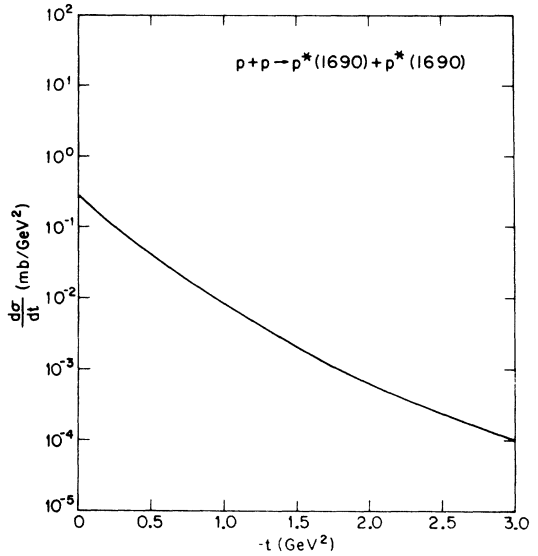

FIG. 5. Coupled-channel double-excitation $pp \to p^*(1690)p^*(1690)$ differential cross section $d\sigma/dt$ vs t.

V. DISCUSSION

The model presented is an optical model of the Chou-Yang type. When the form factors are specified, this model is completely determined. Our procedure was to fix the form factors beforehand and then to confront the results with experimental data. The main guidance in choosing the form factors was the conjecture that the effective form factors of the absorbing matter distribution are similar to the corresponding electromagnetic ones. The results are quite encouraging: All the qualitative features of the data out to $|t| \approx 2$–3 GeV^2 emerge. In particular, we obtain a dip in the elastic differential cross section around $|t| \approx 1$ GeV^2 and no dip in that of the single excitation. In the small-momentum-transfer region, where the model is expected to work best, we find agreement with experiment even to the fine details of the data

such as the change in the slope of elastic scattering.

The model is a phenomenological one, and we have not attempted to justify it by any underlying dynamical scheme. We therefore feel that the main result of this work is to provide some further support to the optical approach in dealing with diffractive scattering of hadrons.

*Work supported in part by the U. S. Atomic Energy Commission under Contracts No. AT(11-1)-3505 and No. AT(11-1)-3066.

†On leave of absence from the Weizmann Institute, Rehovoth, Israel. Present address: Astrophysics Department, Caltech, Pasadena, Calif. 91109.

[1]T. T. Chou and C. N. Yang, Phys. Rev. 170, 1591 (1968); 175, 1832 (1968); in *High Energy Physics and Nuclear Structure*, edited by G. Alexander (North-Holland, Amsterdam, 1967), p. 348.

[2]L. Durand III and R. Lipes, Phys. Rev. Letters 20, 637 (1968).

[3]M. Elitzur, Phys. Rev. Letters 27, 895 (1971).

[4]G. Barbiellini *et al.*, Phys. Letters 39B, 663 (1972). See also M. Holder *et al.*, *ibid.* 35B, 355 (1971); 36B, 400 (1971); U. Amaldi *et al.*, *ibid.* 36B, 504 (1971).

[5]B. T. Carreras and J. N. J. White, Nucl. Phys. B42, 95 (1972).

[6]H. Harari, Ann. Phys. (N.Y.) 63, 432 (1971).

[7]J. V. Allaby *et al.*, Phys. Letters 28B, 229 (1968).

[8]As reported by the Rubbia group at the Sixteenth International Conference on High Energy Physics, N.A.L., Batavia, Illinois, 1972 (unpublished).

[9]E. D. Bloom and F. J. Gilman, Phys. Rev. Letters 25, 1140 (1970); Phys. Rev. D 4, 2901 (1971).

[10]M. Elitzur and L. Susskind, Phys. Rev. D 6, 2003 (1972).

[11]E. W. Anderson *et al.*, Phys. Rev. Letters 25, 699 (1970).

[12]We used Newton's method as an iterative procedure to find κ_{11}, κ_{12}. The calculated σ_T and σ_{exc} rapidly converged within errors to the experimental values. Using $\sigma_T = 38.9 \pm 0.3$ mb and $\sigma_{exc} = 0.56 \pm 0.07$ mb, we found $\kappa_{11} = 10.4$ GeV^{-2} and $\kappa_{12} = 2.41$ GeV^{-2}.

[13]R. M. Edelstein *et al.*, Phys. Rev. D 5, 1073 (1972). The 29.7 resonance excitation data are from this reference.

[14]The 7-GeV resonance excitation data are from C. M. Ankenbrandt *et al.*, Phys. Rev. 170, 1223 (1968); the 19.2 GeV from Ref. 7; the elastic scattering data for constructing the curves from the Particle Data Group compilation, LBL Report No. UCRL-20000*NN*, 1970 (unpublished) and U. Amaldi *et al.*, Phys. Letters 34B, 435 (1971).

PHYSICAL REVIEW D VOLUME 7, NUMBER 5 1 MARCH 1973

Charge Transfer in High-Energy Fragmentation*

T. T. Chou
Department of Physics, University of Denver, Denver, Colorado 80210

and

Chen Ning Yang
Institute for Theoretical Physics, State University of New York, Stony Brook, New York 11790

(Received 9 October 1972)

Nontransference of charge is an essential aspect of the hypothesis of limiting fragmentation for infinite-energy hadron-hadron collisions. One can define experimentally a charge transfer u from one c.m. momentum-space hemisphere to another. At finite energies, u is not zero because the fragments may "spill over" to the other hemisphere. A model is discussed which yields an estimate of u. The general validity of the energy and multiplicity dependence of this estimate is then commented upon.

INTRODUCTION

In the fragmentation picture[1] of high-energy hadron-hadron collisions, the fragments of the target, taken together, have the charge of the target, and similarly for the fragments of the projectile. Define the charge transfer u, an integer, by

$$u = [\tfrac{1}{2}(\text{total charge})_R - \tfrac{1}{2}(\text{total charge})_L]_{\text{final}} - [\tfrac{1}{2}(\text{total charge})_R - \tfrac{1}{2}(\text{total charge})_L]_{\text{initial}}. \quad (1)$$

Here R and L refer to the c.m. momentum-space forward (i.e., projectile) hemisphere and backward